

Influence of toroidal field direction and plasma rotation on pedestal and ELM characteristics in JET ELMy H-modes

A. Loarte¹, G. Saibene¹, R. Sartori¹, M. Kempenaars², R.A. Pitts³, I. Voitsekhovitch⁴, I. Jenkins⁴, J.S. Lönnroth⁵, M. Beurskens⁴, Y. Andrew⁴, V. Parail⁴, E. de la Luna⁶, S. Jachmich⁷, C. Giroud⁴, M.F. Nave⁸, K. Crombe⁹ and JET-EFDA contributors*

¹EFDA CSU-Garching, Boltzmannstrasse, 2, D-85748 Garching bei München, Germany

²Association EURATOM-FOM, FOM Rijnhuizen, P.O. Box 1207, 3430 BE, Netherlands

³CRPP-EPFL, Association Euratom-Confédération Suisse, CH-1015 Lausanne, Switzerland

⁴EURATOM/UKAEA Fusion Association, Culham Science Centre, Abingdon, OX14 3DB, UK

⁵Association EURATOM-Tekes, Helsinki University of Technology, 02015 HUT, Finland

⁶Asociación EURATOM-CIEMAT, Avda. Complutense n. 22, E-28040 Madrid, Spain

⁷LPP, ERM/KMS, Association Euratom-Belgian State, B-1000, Brussels, Belgium

⁸Centro de Fusão Nuclear, Associação EURATOM-IST, 1096 Lisboa Codex, Portugal

⁹Department of Applied Physics, Ghent University, Belgium

1. Introduction.

Experiments have been carried out at JET to determine the influence of the toroidal field direction on L-mode and H-mode plasmas. These included divertor and SOL physics [1] and H-mode physics studies. In this paper we describe the results concerning the influence of toroidal field direction on H-mode plasmas and ELM energy losses, as well as on the operational space of ELMy H-modes. The parameter range explored in these experiments was : plasma current $I_p = 1.2\text{-}3.0\text{MA}$ (with $q_{95} = 3\text{-}3.6$), additional heating (NBI and NBI +ICRH, dominated by NBI) $P_{\text{INPUT}} = 9 - 17$ MW and with various levels of gas fuelling. The discharges had magnetic configurations optimised for ELM power load (DOC-L) and edge pedestal gradient measurements (DOC-U) with an average triangularity $\delta \sim 0.3$. Due to the optimisation of the JET divertor target for power handling, the helicity of the plasma must be preserved and, thus, I_p and B_ϕ were reversed at the same time. Therefore, Forward B_ϕ discharges (FB) had NBI co-injection (and toroidal co-rotation with respect to the I_p direction) while Reversed B_ϕ discharges (RB) had NBI counter-injection (and toroidal counter-rotation with respect to the I_p direction). Comparable FB/RB discharges in steady Type I ELMy H-mode were only achieved at $I_p = 2\text{MA}$, with additional heating at a level of $P_{\text{NBI}} = 11.5\text{-}12.5$ MW + $P_{\text{ICRH}} = 3 - 4$ MW. Discharges at lower plasma current ($I_p = 1.2$ MA) showed density peaking, leading to a radiation increase and the loss of the H-mode for all the explored input power range (up to $P_{\text{NBI}} = 12$ MW). The additional heating was increased up to a level twice that of comparable FB discharges at 1.2 MA, in a failed attempt to avoid the observed peaking. For high plasma current ($I_p = 3\text{MA}$) it was not possible to achieve Type I ELMy H-mode with the available maximum level of additional heating at the time ($P_{\text{NBI}} = 12.3$ MW + $P_{\text{ICRH}} = 3.5$ MW) and the discharges remained in Type III ELMy H-mode. At this level of additional heating, the $I_p = 3\text{MA}$ FB discharges are in the Type I ELMy H-mode with ELM frequencies in the range of 5-10 Hz. Due to the mismatch of the required additional heating to achieve similar Type I ELMy H-modes in FB/RB, our analysis concentrates on the 2MA discharges, for which similar conditions were achieved with both directions of the field (see next Section).

2. Global plasma parameters and pedestal plasma characteristics.

Discharges with overall similar parameters in Type I ELMy H-mode at $I_p = 2\text{MA}$ could be obtained with both directions of the field provided that the level of additional

* See the Appendix of J. Pamela et al., Fusion Energy 2004 (Proc. 20th Int. Conf. Vilamoura, 2004) IAEA, Vienna (2004)

heating was increased by $\sim 20 - 40\%$ for RB discharges (~ 15 MW) with respect to that required to maintain steady Type I ELMy H-modes in similar FB discharges (~ 11 MW). This is in contrast with the required power level to access the H-mode in these experiments, which is similar for both directions of the field [2]. Furthermore, the difference in the heating level required to maintain the Type I ELMy H-mode with RB cannot be attributed to increased beam losses associated with counter injection. These are due to the ionised beam neutrals following banana orbits in the outwards direction, which intersect the main chamber plasma facing components (PFCs) for counter injection discharges. In order to avoid overheating the PFCs with such losses, RB discharges at JET were run with a larger clearance from the main wall (~ 10 cm at the outer midplane instead of 3-5 cm for similar FB discharges) and this maintained similar beam losses (in the range of 2-5% of P_{NBI}) for comparable RB/FB discharges, as estimated by TRANSP modelling.

Once the level of additional heating is high enough to achieve discharges in steady-state Type I ELMy H-modes in RB, the JET discharges themselves are quite comparable, as shown in Fig. 1 for the ELM frequency and Fig. 2 for the plasma energy. The major difference between RB and FB discharges concerns the plasma density, which is significantly lower (by 20 to 40%) and the plasma energy which is slightly lower (by $\sim 10\%$) for RB discharges (with similar P_{INPUT} and gas fuelling level) in the Type I ELMy H-mode. The plasma density and plasma energy become again similar for both directions of the field once the discharge enters the Type III ELMy H-mode, indicating that the direction of the field (or plasma rotation) affects more strongly the edge plasma in the Type I than the Type III ELMy H-mode regime. The differences in core plasma energy and particle content in FB/RB discharges are correlated with differences in pedestal plasma parameters, as shown in Fig. 3. RB discharges have a pedestal pressure which is 20 - 30% lower than similar FB plasmas, mostly because the lower pedestal density in RB discharges. The ratio of pedestal energy to total plasma energy ($W_{\text{ped}}/W_{\text{dia.}}$) in RB discharges is ~ 0.33 , which is virtually the same as FB discharges with similar levels of input power [3]. As a consequence, the energy confinement time for the core plasma (subtracted the pedestal contribution) is the same in RB and FB discharges and the lower global energy confinement in RB discharges can be attributed to the differences in the pedestal plasma energy. These results resemble closely those obtained in similarity experiments between JET and JT-60U. In that case the differences have been attributed to toroidal field ripple (and/or rotation) differences between the two devices [4].

3. ELM energy losses and edge MHD stability.

Due to the lower pedestal energy in RB discharges, it is expected that the ELM energy losses would be smaller in absolute magnitude than those of comparable FB discharges, which is indeed seen in the experiment. Furthermore, the ELM energy losses in RB discharges are smaller than those in FB pulses even when they are normalised to the pedestal energy, $\Delta W_{\text{ELM}}/W_{\text{ped}}$, as shown in Fig. 4. For RB, $\Delta W_{\text{ELM}}/W_{\text{ped}}$ deviates clearly from the trend of ELM energy losses to increase with decreasing density (or pedestal collisionality) [5]. $\Delta W_{\text{ELM}}/W_{\text{ped}}$ is very small ($\sim 10\%$) for RB, even at very low values of pedestal density and collisionality ($n_{\text{ped}}/n_{\text{Greenwald}} \sim 0.25$, $v_{\text{ped}}^* \sim 0.03$, the latter being similar to that expected in ITER [3]). The reason for the different behaviour in RB and FB discharges is the difference in the perturbation that ELMs cause to the edge pedestal temperature for the two directions of the field, as shown in Fig. 5. FB discharges at low plasma density show large perturbations to the electron pedestal temperature following the

ELMs (20 - 40% drop). This perturbation decreases with increasing plasma density and this is associated with the change in the dominant ELM energy loss mechanism from conduction to convection [3]. However, for RB discharges, the pedestal temperature drop caused by the ELMs is very small (10 – 15 %) even at the lowest densities and is weakly dependent on plasma density. In contrast, the area of the plasma which is subject to the perturbations by the ELMs is similar for both directions of the field (20-25 % of the plasma radius) and weakly dependent on the plasma density. The characteristics of the ELM energy losses determined in these RB discharges resemble quite closely those of the low collisionality convective ELMs observed at JET high δ (~ 0.45 - 0.5) and high q_{95} ($\sim 4.5 - 5.0$) discharges, which are compatible with ITER PFCs lifetime requirements [3]. This indicates that the achievement of these convective ELMs at ITER-like collisionalities is not linked to a particular plasma configuration, rather to features of the edge plasma stability, which can be obtained in various operation scenarios.

Initial studies of MHD stability for comparable FB/RB discharges have been carried out based on the experimentally measured edge density and temperature profiles with the modelling tools available at JET [6]. These studies show that comparable FB/RB discharges in terms of input power and gas fuelling (with similar T_{ped}) have similar edge gradients (within the resolution of the edge diagnostics at JET). Therefore, the operation points in the edge stability diagram are located very close to each other (normalised pressure gradient lower by 10% for RB), as shown in Fig. 6. It is important to note that the absolute magnitude of the gradients in RB/FB are similar, despite the pedestal pressure in RB being 30% lower than in FB. This is mostly due to differences in the edge density profile for RB discharges, which is narrower than for FB discharges, as indicated by a larger database of measurements for FB and RB discharges with the JET edge LIDAR diagnostic.

4. Conclusions.

Access to the Type I ELMy H-mode at JET with Reversed B_{ϕ} (and I_p) requires a $\sim 30\%$ more additional heating power than in Forward B_{ϕ} discharges, which cannot be explained by enhanced beam losses with RB. Comparable FB/RB discharges in Type I ELMy H-mode differ mostly in the plasma density, lower for RB discharges, leading to a lower pedestal pressure for RB. The differences between RB and FB discharges are much smaller in the Type III ELMy H-mode, indicating that the direction of the field (or counter-injection/counter rotation) has a stronger effect on the pedestal stability for the Type I ELMy H-mode. Type I ELMs in RB discharges are small and cause very small perturbations of the pedestal temperature ($\sim 10\%$) even at ITER-like pedestal collisionalities, i.e., they are convective ELMs. Measurements of the edge pressure gradients and MHD stability studies indicate that both are similar for comparable FB/RB discharges. The differences in absolute pressure at the pedestal top for RB discharges is, thus, caused by a smaller edge pressure scale length (mostly due to the edge density) in RB discharges. The reasons for the narrower edge density profile in RB remain to be understood and could be linked to the changes in ion losses from the plasma edge region (and/or of counter-injected ions) and edge flows with B_{ϕ} direction or to the effects of plasma rotation on edge stability, which have not been considered in this study. Understanding the physical mechanisms behind the low collisionality convective ELMs obtained in the RB experiments could provide important information for the realisation of such ELMs in ITER.

5. References.

- [1] Pitts, R.A., et al., *J. Nucl. Mat.* **337-339** (2005) 146. [2] Andrew, Y., et al., *Plasma Phys. Control. Fusion* **46** (2004) 337.

[3] Loarte, A., et al., Phys. Plasmas **11** (2004) 2668. [4] Saibene, G., et al., Plasma Phys. Control. Fusion **46** (2004) A195.
 [5] Loarte, A., et al., Plasma Phys. Control. Fusion **44** (2002) 1815. [6] Lönnerth, J.S., et al., Plasma Phys. Control. Fusion **46** (2004) 1197.

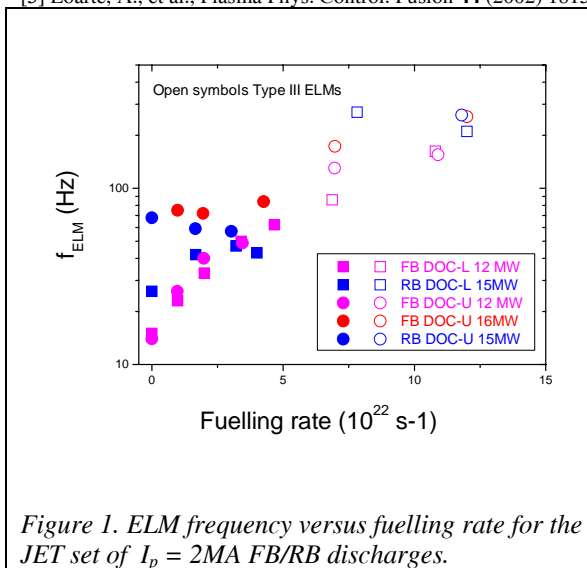


Figure 1. ELM frequency versus fuelling rate for the JET set of $I_p = 2MA$ FB/RB discharges.

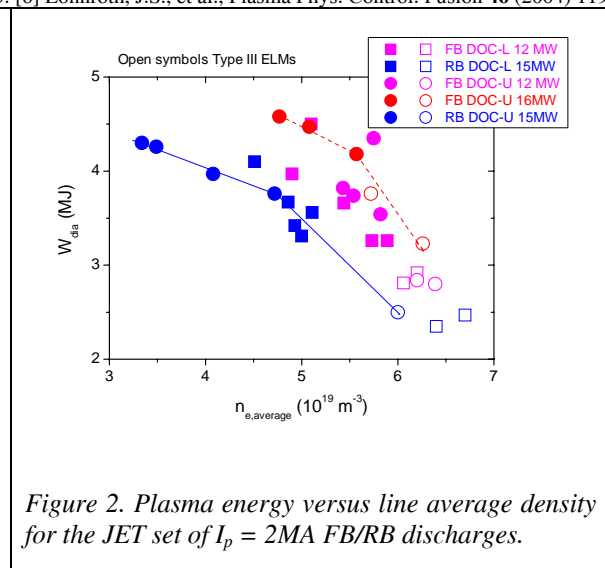


Figure 2. Plasma energy versus line average density for the JET set of $I_p = 2MA$ FB/RB discharges.

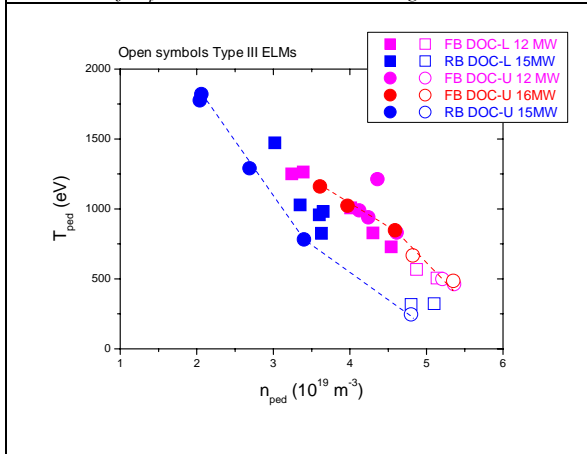


Figure 3. Pedestal electron temperature versus pedestal plasma density for the JET set of $I_p = 2MA$ FB/RB discharges.

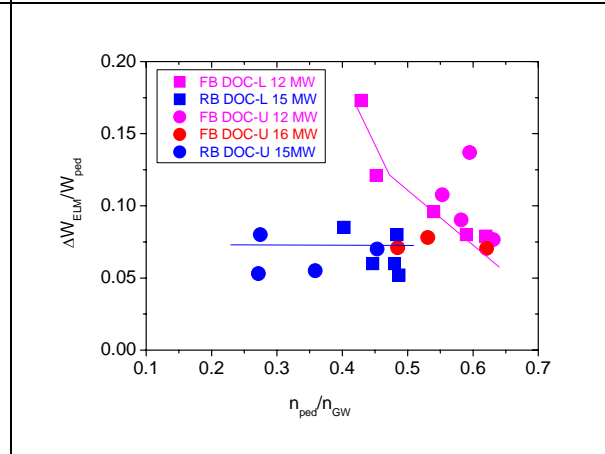


Figure 4. Normalised (to the pedestal energy) Type I ELM energy loss versus normalised (to the Greenwald density) pedestal plasma density for the JET set of $I_p = 2MA$ FB/RB discharges.

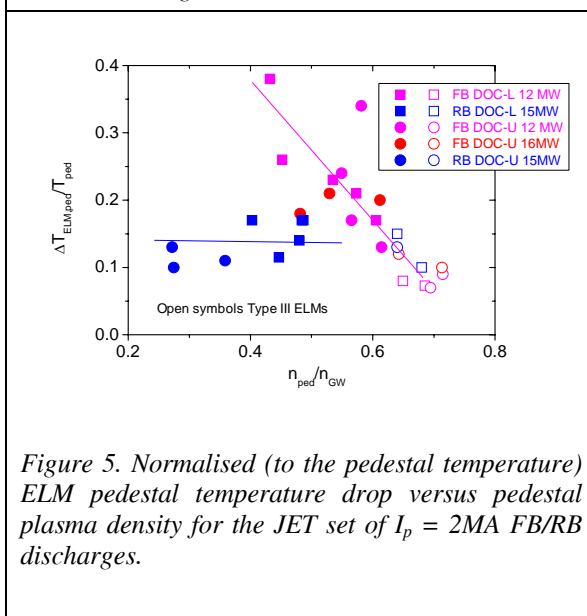


Figure 5. Normalised (to the pedestal temperature) ELM pedestal temperature drop versus pedestal plasma density for the JET set of $I_p = 2MA$ FB/RB discharges.

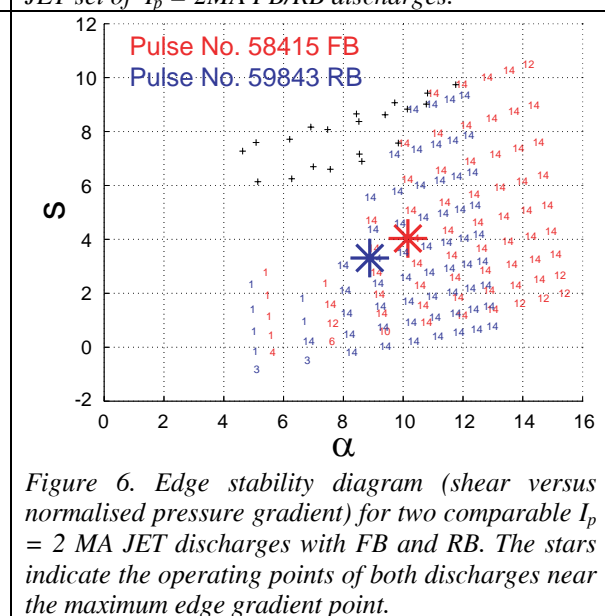


Figure 6. Edge stability diagram (shear versus normalised pressure gradient) for two comparable $I_p = 2 MA$ JET discharges with FB and RB. The stars indicate the operating points of both discharges near the maximum edge gradient point.